J. Astrophys. Astr. (1982) 3, 39–61

A Study of the H-Alpha Line in Late G and K Supergiants

Sushma Vasu Mallik *Indian Institute of Astrophysics, Bangalore 560034*

Received 1981 September 24; accepted 1982 February 5

Abstract. A spectroscopic study of H_α has been carried out to investigate the properties of expanding chromospheres of late G and K supergiants. Spectra of 23 stars brighter than $V = 6{\cdot}0$ have been obtained at dispersions of 4–10 Å mm^{-1} using the coudé and the coudé-echelle spectrographs at the 102-cm telescope of Kavalur Observatory. The H_α profiles are all asymmetric in the sense that the absorption core is shifted to the blue by amounts ranging between − 4 and − 24 km s^{-1}.

H_α profiles were theoretically computed using radiative transfer in spherically symmetric expanding atmospheres covering a large range of integrated optical depths. These were compared with the characteristics of the observed line in the programme stars. The analysis shows that the H_α line is formed in a region with velocity increasing outward. The computed equivalent widths and line core displacements were matched with those observed to obtain hydrogen column densities and expansion velocities. From these, the rates of mass loss in these stars were determined to be in the range of 10^{-6}–$10^{-7} M_\odot$ yr^{-1}.

Key words: late-type stars—chromospheres—mass loss

1. Introduction

The existence of chromospheres has been well indicated by the presence of Ca II H (λ 3968) and K (λ 3934) emission in late-type stars. The H and K emission components designated as H_2 and K_2, are present in several F stars, in most of the G stars and in all the K and M stars that have been observed (Joy and Wilson 1949; Bidelman 1954; Wilson and Bappu 1957; Warner 1966, 1968, 1969; Wilson 1976). Other spectroscopic features of chromospheric origin include lines of Mg II (h and k), H I (L_α and H_α), He I (λλ 10830, 5876) and O I, Si II and Fe II in the far ultraviolet (Linsky 1980).

The chromospheric emissions in Ca II H and K, particularly in giants and supergiants, show a central absorption reversal. The cores of these absorption components (designated as H_3 and K_3) are displaced to the blue with respect to the 'photospheric' line centre (Deutsch 1956, 1960; Reimers 1975, 1977; Boesgaard and Hagen 1979) suggesting a net outward motion of the regions of the atmosphere where these lines are formed. Both the chromosphere and the circumstellar envelope contribute to the central absorption reversal. The violetshifted absorption cores along with similar asymmetries detected in many other resonance lines and lines of low excitation potential, have been widely used to determine physical conditions in the circumstellar envelopes of M giants and supergiants in particular, and also to derive the rates of mass loss from their envelopes (Sanner 1976; Bernat 1977; Hagen 1978). At the same time, it has also been found that the emission components K_2 in the same stars are blueshifted with respect to the line centre which indicates that the chromospheres themselves may be expanding (Stencel 1978). Bappu (1981) has studied the relative velocity shifts of Ca II chromospheric emission ΔE and absorption Δa in several stars and has classified the stars according to the chromospheric emission differential velocity. For stars with large negative ΔE ($\Delta E \leqslant -2$ km s^{-1}), he has found that those with $\Delta a - \Delta E \leqslant -2$ km s^{-1} are in the region of large wind outflow which indicates once more that for a fraction of the stars, expansion starts at chromospheric levels.

Unlike the case of M supergiants, the observational data on late G and K supergiants are rather scanty. Reimers (1977) found that the Ca II K_3 and H_3 components in late G and K supergiants showed high time variability in strength as well as in line-core displacement. Therefore, no meaningful mass-loss rates could be derived for these stars. Information from other lines (*e.g.* Ti II $\lambda\lambda$ 3659, 3383) is not available either (Reimers 1977).

Most of the circumstellar lines in late-type supergiants lie in the violet part of the spectrum, where these stars are quite faint. A survey in the red has the advantage that a much larger sample of them extending to fainter magnitudes can be studied. Weymann (1962) had noticed a distinct asymmetry in the profiles of the Balmer lines of α Ori. Kraft, Preston and Wolff (1964), in their study of H_α core widths in late-type stars, also observed that H_α line cores in most of the K supergiants are shifted to the blue. They also detected in some of the stars small emission components on the blue or on the red side of the absorption profile lying above the level of the continuum. More recently, Cohen (1976) and Mallia and Pagel (1978) have found blueshifted H_α absorption cores and weak emission components in the K giants of some globular clusters. Since the bulk of the H_α absorption is known to occur in the chromospheres (Athay and Thomas 1958), the H_α observations are interpreted as indicative of expanding chromospheres. Goldberg (1979) has recently confirmed Weymann's measurements of the violet displacement of the H_α core in α Ori. His results strengthen further the premise that the bulk of H_α is formed in the innermost layers of the expanding outer atmosphere, *i.e.* the chromosphere itself. A study of H_α is likely to yield information on the layers where the expansion begins and to provide better insight into the mass-loss phenomenon. Boesgaard and Hagen (1979), in their study of the circumstellar shells of M giants, found the H_α line to be asymmetric in many of them. Since H_α is a strong line in G and K supergiants and since the stellar continuum is also bright in the neighbourhood of H_α, the H_α line is a powerful tool for the analysis of expanding chromospheres of these stars.

Moreover, since H_α is the only line in the visual spectrum that has both a large opacity and a large scale-height in the chromosphere (Athay 1976), it can probe the chromosphere over a large extent.

In the present study the H_α line was observed in 23 supergiants brighter than $V = +6{\cdot}0$ ranging in spectral types from G8 to K7. Theoretical H_α profiles were computed and were used to fit the gross characteristics of the observed line, particularly, their equivalent widths and core displacements. Thus the column densities and velocities were determined. Finally, rates of mass loss from the expanding chromospheres of these stars were derived assuming a steady-flow situation.

The observations and the methods of reduction are discussed in Section 2. In Section 3, the theoretical framework for the analysis of the line profiles and also the results are given.

2. Observations

2.1 *The Programme*

Twenty-three stars brighter than $V = +6{\cdot}0$ were sampled in the range of spectral types G7 Ib through K7 Ib from the Bright Star Catalogue (Hoffleit 1964) and the list of supergiants given by Humphreys (1970). Basic data for the programme stars are given in Table 1.

Table 1. Data for programme stars.

Star HR	Star HD	Name	Spectral type	V	M_V
237	4817		K5 Ib	6·07	
834	17506	η Per	K3 Ib	3·76	−3·8
861	17958		K3 Ib	6·51	
2473	48329	ϵ Gem	G8 Ib	3·08	−4·5
2580	50877	o^1 CMa	K3 Iab	3·78	−4·7
2615	52005	41 Gem	K4 Ib	5·62	−3·1
2646	52877	σ CMa	M0 Iab	3·46	−4·2
2764	56577		M0 Ib	4·83	−4·1
2993	62576		K5 Ib	4·58	−4·3
3225	68553		K3 Ib	4·44	
3612	77912		G7 Ib-II	4.60	−2·2
3634	78647	λ Vel	K5 Ib	2·30	−3·8
3692	80108		K3 Ib	5·11	
4050	89388		K5 Ib	3·39	−3·7
4120	91056		K3 Ib	5·26	
5742	137709		K5 Ib	5.25	
6461	157244	β Ara	K3 Ib	2·84	−4·0
7114	174947	33 Sgr	K0 Ib	5·75	
7866	196093	47 Cyg	K5 Ib	4·72	
8079	200905	ξ Cyg	K5 Ib	3·72	−2·0
8308	206778	ϵ Peg	K2 Ib	2·42	−4·1
8465	210745	ζ Cep	K1 Ib	3·35	−4·7
8726	216946		K5 Ib	4·98	−4·4

Fourteen of the twenty-three stars have been observed to have chromospheric Ca II H and K emission. For twelve of these, the absolute magnitudes were taken from Wilson (1976) and for the other two stars, HD 89388 and β Ara, from Warner (1969). The value of M_V for HD 62576 was obtained from Luck (1977).

The absolute bolometric magnitudes and hence luminosities for these stars were calculated using the bolometric corrections of Johnson (1966). The effective temperatures are known only for nine of them (Luck 1977, 1979). The radii obtained for these nine using the relation $L = 4\pi R^2 \sigma T_{\rm eff}^4$ are in the range of $(1{\cdot}0 \pm 0{\cdot}5) \times 10^{13}$ cm.

2.2 *Coudé Spectrograms*

Spectrograms of λ Vel, η Per and o^1 CMa were obtained on Kodak 098–02 emulsion at the coudé focus of the 102-cm telescope at Kavalur Observatory using the 112-in camera and a 400 g mm^{-1} grating. The reciprocal dispersion was 4·2Å mm^{-1} in the second order and the resolution on the plate 0·13 Å. The spectral range covered was from 6200 Å to 6800 Å.

Another set of spectrograms was obtained for all the twenty-three programme stars with an echelle spectrograph at the coudé focus of the same telescope using a 7-in camera and an uncooled single stage Varo image tube. The spectrograph had a 79 g mm^{-1} echelle grating, blazed at 6745 Å in the 34th order which contained the H_α line and the dispersion in that order was 10·5 Å mm^{-1}. The positions of the echelle grating and of the cross-disperser were adjusted such that on each echellogram, the H_α line was in the centre of the field of view. The observed spectrum ranged from 5200 Å to 7800 Å. It was clear from the density tracings obtained of the above spectrograms that the deepest part of the H_α line is shifted shortward of the rest line centre producing a distinct asymmetry.

2.3 *The Reduction Procedure*

It is hard to locate the deepest part of the line on the plate itself because the H_α line is quite broad. So, instead of measuring the position of the line core on the comparator, we have determined it on the density tracing of each star. The dispersion is nonlinear along any single order. An independent measurement showed that a second degree polynomial fits well the relationship between the wavelength and the distance. This scale was determined on each density tracing and the position of the H_α line core located with the aid of the adjacent photospheric Fe I lines. The displacements measured in units of wavelengths are then expressed in units of velocity. The accuracy of the measurements is about 1 km s^{-1} as determined from the error involved in measuring the position of the H_α core. The displacements obtained with respect to the three Fe I lines differ by less than 1 km s^{-1}. Hence the internal accuracy of the measurement is $\leqslant 1$ km s^{-1}.

A few representative density profiles are shown in Fig. 1. The density profiles were converted into intensity profiles using the calibration spectra. Fig. 2 shows the intensity profiles corresponding to the density profiles in Fig. 1. The equivalent widths

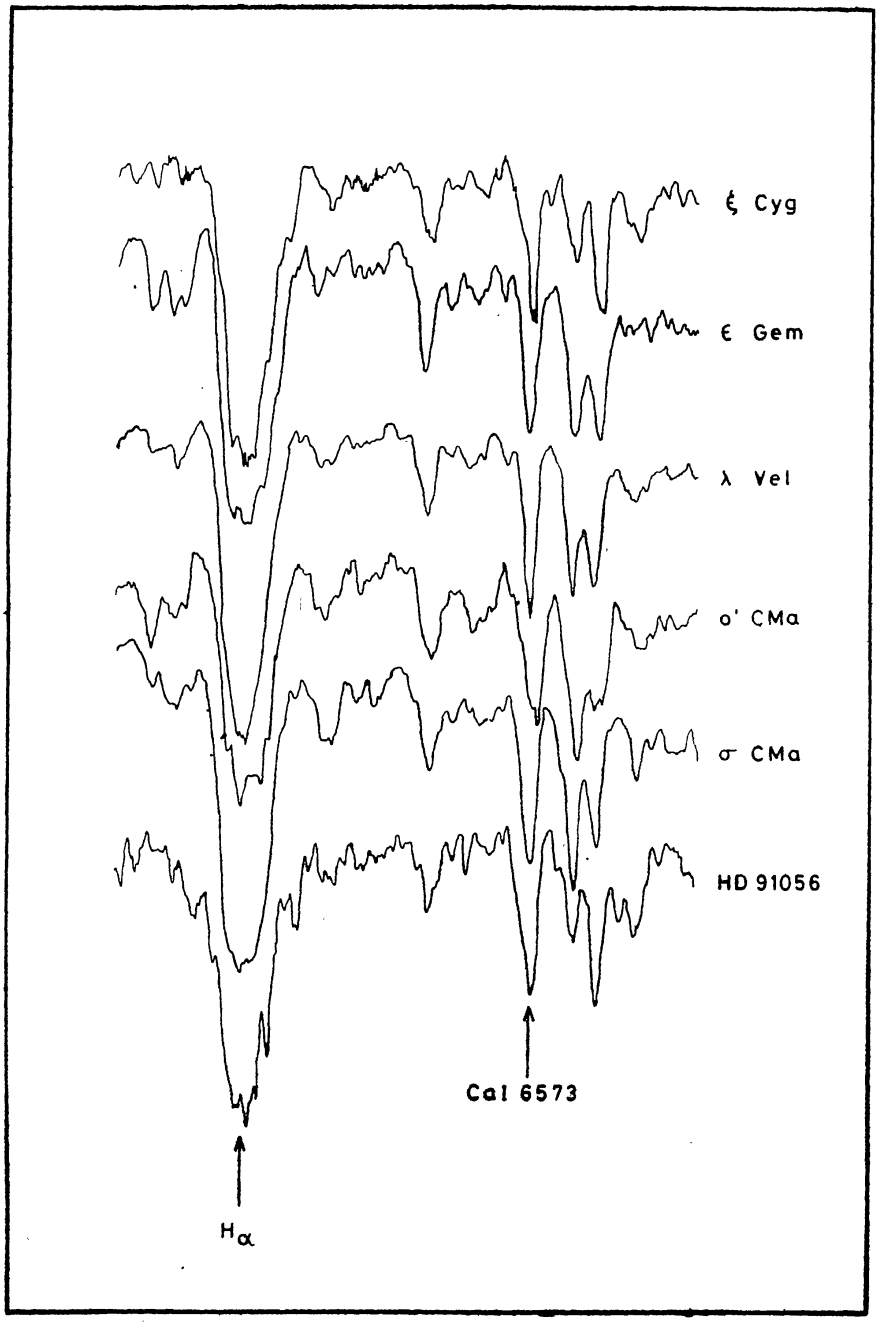

Figure 1. Density profiles of H_α in representative G and K supergiants.

determined from the different intensity profiles of the same star agree to within 10–15 per cent (or $\pm$ 0·2 Å). The equivalent widths (EQW) and the line-core displacements (LCD) listed in Table 2(a) are the averages over the number of spectra obtained for each star as given in column (2) of the table. Table 2(b) gives the H_α velocity displacements and the EQWs for the three stars λ Vel, o^1 CMa and η Per observed at the coudé spectrograph. The EQWs and the LCDs obtained in the two cases differ by less than 10 per cent.

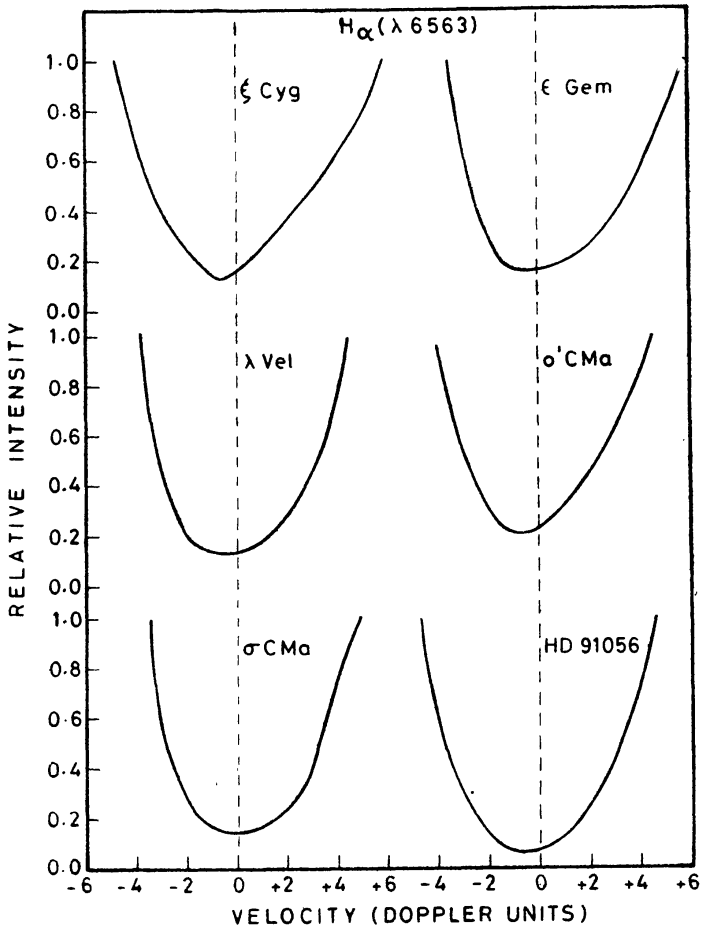

Figure 2. Intensity profiles of H_α corresponding to the density profiles in Fig. 1.

2.4 *Correlations between the Observed Quantities*

Deutsch (1956, 1960), in his study of the Ca II circumstellar lines in red giants, found strong correlations between (a) the spectral type and the strength of the H_3 and K_3 lines and (b) the strength and the expansion velocity of H_3 and K_3. According to him, H_3 and K_3 increased in strength and the expansion velocities decreased in the later spectral types. Deutsch attributed these trends to either a decrease in the amount of matter in the envelope and/or an increase in the ionization from the observable Ca II to Ca III. Although the ionization of H is insensitive to the range of temperatures involved here, it is worth investigating if similar correlations exist for the H_α line. In Figs 3 and 4, we have plotted the H_α strengths and velocities against the spectral type. It is seen that neither the strength of the H_α line core nor its position is related to the spectral type. The same result was obtained by Boesgaard and Hagen (1979) for the H_α line in M giants.

Table 2. H_α strengths and velocities.

(a) Coudé echelle spectra:

Star	Spectral type	No. of spectrograms n	Shift of the H_α line core (km s^{-1})	EQW of the H_α absorption (Å)
HD 77912	G7 Ib	2	−13·4	1·33
ϵ Gem	G8 Ib	2	− 8·1	1·77
33 Sgr	K1 Ib	1	− 4·9	1·67
ζ Cep	K1 Ib	2	−13·8	1.81
HD 196093	K2 Ib	1	−18·6	1·34
ϵ Peg	K2 Ib	2	− 8·7	1·80
η Per	K3 Ib	3	− 7·5	1·84
HD 17958	K3 Ib	1	−17·2	1·27
σ^1 CMa	K3 Iab	3	− 6·9	1·22
41 Gem	K3 Ib	3	− 9·2	1·36
HD 56577	K3 Ib	4	− 6·1	1·47
HD 62576	K3 Ib	2	−15·4	1·23
HD 68553	K3 Ib	3	−30·1	1·51
HD 80108	K3 Ib	1	−21·4	1·68
HD 91056	K3 Ib	1	− 8·7	1·98
β Ara	K3 Ib	7	−18·3	1·60
HD 4817	K5 Ib	1	−12.0	1·81
λ Vel	K5 Ib	3	−11·8	1·66
HD 89388	K5 Ib	1	−22·9	1·79
HD 137709	K5 Ib	3	− 9·3	1·69
ξ Cyg	K5 Ib	2	− 9·3	1·93
σ CMa	K7 Iab	3	−10·6	1·72
HD 216946	M0 Ib	2	−17·1	1·83
(b) Coudé spectra:				
η Per	K3 Ib		− 5·1	1·76
σ^1 CMa	K3 Iab		− 7·2	1·35
λ Vel	K5 Ib		−10·2	1·72

3. Analysis of the line profiles

3.1 *Theoretical Framework*

Because of their vast extent, the atmospheres of supergiants cannot be properly described by the classical plane-parallel LTE model atmospheres. Therefore, until recently, it was not possible to interpret adequately the observational data relating to the supergiant atmospheres. Only in the last few years, the theory of radiative transfer in extended and spherically symmetric expanding atmospheres has been worked out in some detail and models have become available (Kunasz and Hummer 1974; Mihalas 1978 and the references contained therein). A different formulation of the same problem has been given by Peraiah and Grant (1973) and Peraiah (1979, 1980, 1981) in the framework of the discrete space theory of radiative transfer. With these theoretical advances it is now possible to interpret and model the observations to a much fuller extent.

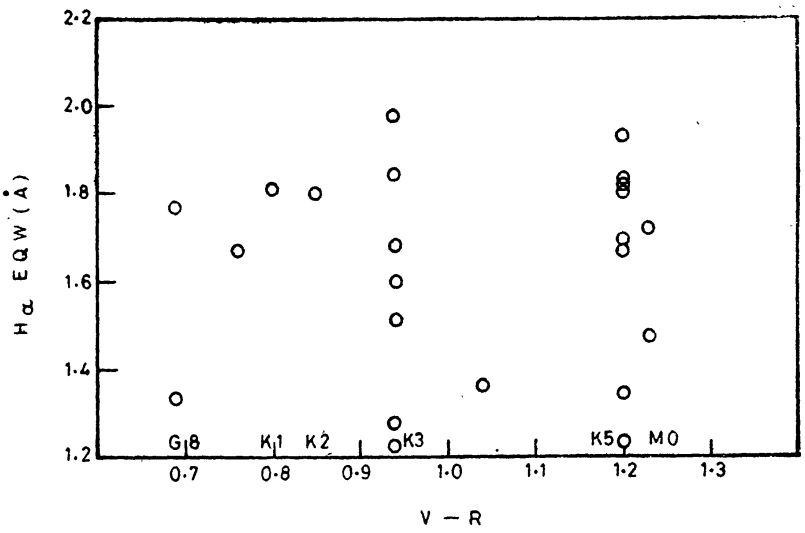

Figure 3. H_α equivalent width versus spectral type. The corresponding $V-R$ values are from Johnson (1966).

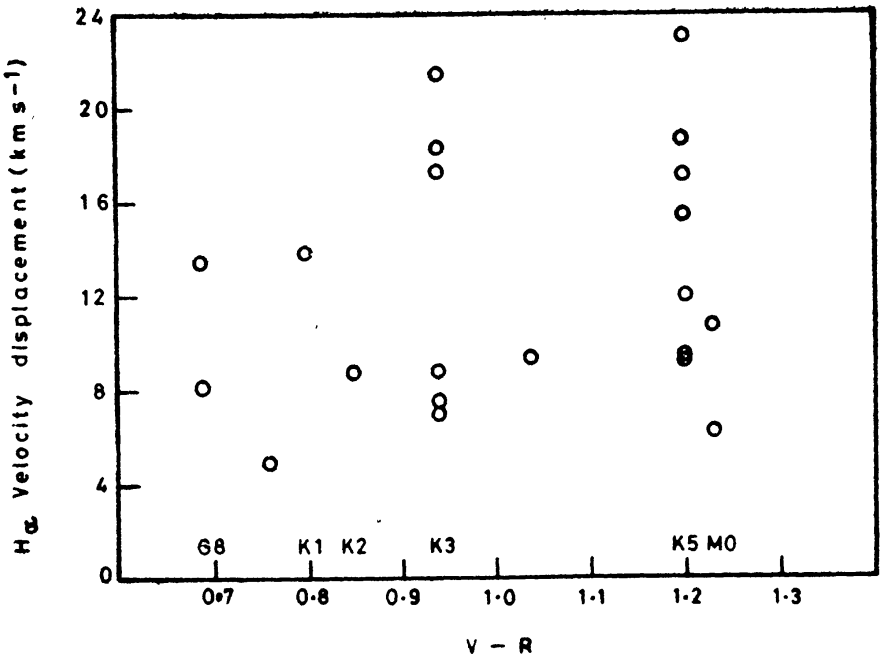

Figure 4. H_α velocity displacement versus spectral type.

The H_α line source function obtained by solving the equation of radiative transfer in the chromosphere can be used to simulate the theoretical line profiles for an observer at infinity. The gross characteristics of the observed line, the equivalent width and the core displacement in particular, are then compared with these theoretical profiles to obtain data on column densities and velocity structure of the line-forming region.

In the present work, the line source function was adopted from the work of Peraiah (1981) where the solution of the equation of radiative transfer has been given for the case of an expanding atmosphere. The line source function, S_l, is written as

$$S_l(x, \pm\mu, r) = (1-\epsilon)\int_{-\infty}^{\infty} dx' \int_{-1}^{1} \phi(x')\, I(x', \mu')\, d\mu' + \epsilon\, B(r) \qquad (1)$$

where $I(x', \mu')$ is the specific intensity of the ray making an angle $\cos^{-1}\mu'$ with the radius vector r and with frequency $x' = (\nu - \nu_0)/\Delta\nu_D$, $\Delta\nu_D$ being the Doppler width; ϵ is the destruction probability of photons via collisions, ϕ is the profile function and $B(r)$ is the continuum intensity which is set equal to the Planck function. The calculation of the source function was based on:

(i) a two level atom without continuum,
(ii) Doppler profile function,
(iii) the density of the absorbing material decreasing linearly with r,
(iv) the velocity increasing linearly with r with V_{max} at the outer radius equal to 10 thermal units, and
(v) ϵ set equal to zero. $\epsilon = 0$ is particularly suited to the case of H_α because it is a photo-ionization dominated line (Jefferies and Thomas 1959). With a non-zero ϵ, the line source function leads to profiles with a prominent central emission (Peraiah 1981), contrary to the observed H_α flux profiles. Further, the ratio of the continuum to line opacity, β, was assumed to be zero.

In the present work, we are dealing with large integrated optical depths in order to obtain the strong absorption profiles, as observed in the programme stars. Since the bulk of the absorption occurs within a narrow region near the inner boundary in the case of a decreasing density distribution, the source function with $\epsilon = \beta = 0$ and large τ is particularly insensitive to either the thickness of the line-forming region (so long as it is not too large) or the assumed density distribution across it.

The boundary conditions on the specific intensities incident on either side of this region are: (a) the radiation incident on the inner boundary is the Planck radiation field of the star $B(r)$ and (b) there is no radiation incident on the outer boundary.

3.2 *Geometry of the Problem*

In previous studies, which have mostly been of circumstellar shells of M giants and supergiants (Weymann 1962; Sanner 1976; Bernat 1977; Hagen 1978; Boesgaard and Hagen 1979), low densities and hence low optical depths were involved. In the case of H_α where the bulk of the absorption takes place in the chromosphere, the inner boundary of the line-forming region is the photosphere itself, in other words, the radius of the star. Consequently, much higher densities and optical depths are encountered. Since the theoretical framework used here could tackle large optical depths, it was possible to treat the H_α line-formation problem satisfactorily. The inner boundary was assumed to be 10^{13} cm for all the stars, based on the calculations for nine of them. At present, there exists no observational clue to the extent of the H_α line-

forming region in late-type giants. It is expected, however, that at greater heights in the chromosphere where temperatures are higher than 10,000 K, there is no appreciable neutral hydrogen (Linsky 1980; Athay 1976). In any case, since the radiation field becomes rather dilute at greater heights, it is hard to imagine that the $n = 2$ level of H is populated sufficiently there. This is supported by the recent study of the H_α line in M giants by Boesgaard and Hagen (1979) where they find that H_α formation is confined to a narrow region near the inner boundary. The velocity and density distributions adopted here satisfy the equation of continuity in the plane-parallel limit. Therefore, in the present analysis, the extent of the line-forming region, ΔR, was adopted to be a small fraction of the stellar radius. The line-forming region was divided into a number of shells. The discretised coordinate used in the programme was the shell number which varied from 1 to 90 over the extent of the envelope. The shell number is a linear function of the radial distance from the centre of the star. The frequency was discretised in units of the Doppler width $\Delta\nu_D$ in the same way as the velocity was expressed in thermal units V_{th}. Since the absorbing matter is assumed to expand with a velocity linearly proportional to radius which is discretised in terms of the shell number, the velocity was also assumed to grow in the atmosphere in a discretised fashion in the following way:

$$V_n = V_a + \frac{V_b - V_a}{N}(n - 1 + \tfrac{1}{2}) \tag{2}$$

where V_a is the velocity at the inner edge of the line-forming region and V_b the velocity at its outer edge and N the total number of shells. The source function adopted is displayed in Fig. 5 as a function of the optical depth. It is seen that $S(r)$ drops down by almost four orders of magnitude over the extent of the envelope.

With the velocity $v(r)$, the density $n(r)$ and the source function $S(r)$ specified at each shell, the computation of the line flux as a function of frequency is fairly

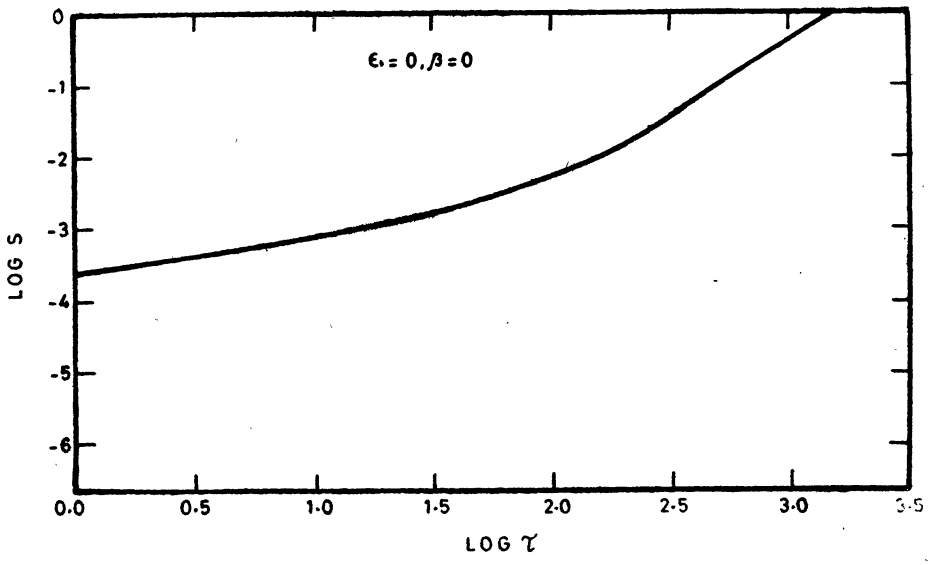

Figure 5. Source function as a function of the optical depth.

straightforward. The material behind the star is hidden from the observer and that in front gives rise to absorption (Fig. 6). The flux F'_ν due to this absorption is calculated at infinity for each frequency by the observer. In the two emission lobes on either side of the absorbing region, velocities in different radial directions contribute differently to the line of sight components of intensities. The intensities of rays for a given frequency, along the line of sight of an observer at infinity are calculated at equally spaced radial points of interval h perpendicular to the line of sight. The flux is calculated by integrating over all such intensities throughout the shell bounded by $R_{\rm in}$ and $R_{\rm out}$. The flux in each lobe is given by

$$F_\nu = 2\pi \int_{R_{\rm in}}^{R_{\rm out}} I_\nu (h)\, h\, dh. \tag{3}$$

As the two emission lobes are identical the total flux received at infinity is given by

$$f_\nu = F'_\nu + 2\, F_\nu. \tag{4}$$

3.3 *Optical Depth and Column Density*

The optical depth at the centre of the H_α line is

$$\tau_0 = \frac{\sqrt{\pi}\, e^2}{mc} \frac{f}{\Delta\nu_{\rm D}} N' = \alpha'\, N' \tag{5}$$

where e, m and c are the electronic charge, the electronic mass and the velocity of light respectively and f is the oscillator strength for the H_α transition and is 0·64

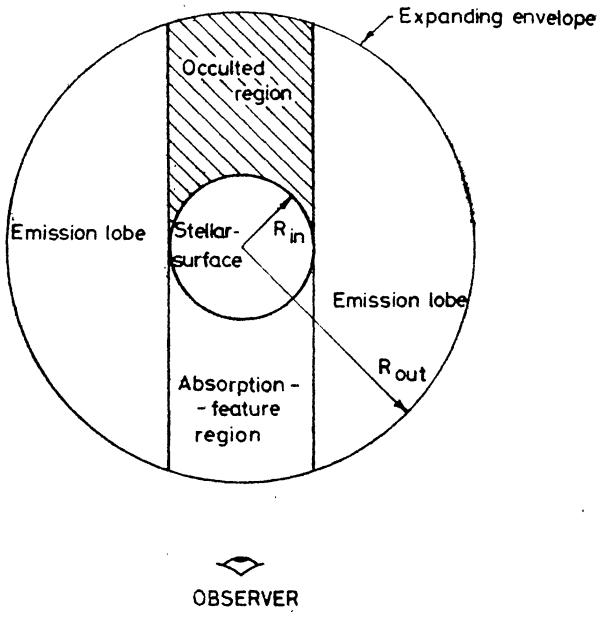

Figure 6. Schematic diagram of the expanding envelope.

(Wiese, Smith and Glennon 1966). N' is the column density of the line-forming atoms and may be written as

$$N' = \int_{R_{in}}^{R_{out}} n_2 dr = \int_{R_{in}}^{R_{out}} \delta n dr \qquad (6)$$

where n_2 is the number density of H in the second level and n is the total number density of H. To simulate the overpopulation of the second level of H in the chromosphere, a temperature T was used in calculating δ which was higher than T_{exc} determined by Luck (1977, 1979) for many of the G and K supergiants studied here. According to Mihalas (1978), H_α is formed at depths in the solar chromosphere where T is about 5500 K. In their chromospheric model of α Boo, Ayres and Linsky (1975) find T varying from 4000 to 10,000 K. A temperature of about 5000–5500 K in this model occurs at depths where the number density of hydrogen is in the range 10^{11}–10^{12} cm^{-3}, typical of the middle chromosphere where H_α is likely to be formed. In the present work a temperature of 5500 K was assumed for the H_α forming region of the chromospheres of all the G and K supergiants. Using this value, the fraction δ was calculated. The expression for τ is then

$$\tau = \alpha' \delta N \equiv \alpha N \qquad (7)$$

where N is the total column density of H. The population of the level $n = 2$ is quite unknown for the programme stars because of a lack of knowledge of the temperatures and the non-LTE factors in the chromosphere. Therefore, τ itself was used as a parameter in the computations.

3.4 *Microturbulence*

In stellar atmospheres the width of an absorption line has contributions from thermal Doppler broadening as well as microturbulence. According to Kuhi (1974), the root-means-quare turbulence ξ_t may be as large as 18 km s^{-1} or higher in supergiants. Boesgaard and Hagen (1979) deduce almost as large a value for microturbulence for late-type supergiants. Ayres and Linsky (1975) find for α Boo, an optimum value of 12·5 km s^{-1} in the chromosphere. Since the width of the line at the continuum level and hence the equivalent width are dependent upon ξ_t it was used as a free parameter in the line profile calculations. No depth dependence of microturbulence was taken into account. A higher ξ_t leads to a lower optical depth in the line for a given density.

3.5 *Computation of Line Fluxes*

With the source function given in Fig. 5 and the adopted density and velocity distributions [$n(r) \propto (1/r)$ and $v(r) \propto r$], theoretical H_α profiles were computed covering a large range of integrated optical depths. Each computer run of a set of theoretical profiles was characterised by a density and a velocity at the inner radius, a turbulent velocity and the extension of the envelope. Each profile in the set was characterised by a particular value of the velocity at the outer radius. The LCD and

the EQW were determined for each profile. The inner velocity was varied to obtain different series of computed profiles. With a higher inner velocity for the same outer velocity, the LCD was higher and the EQW lower. Since most of the observed profiles have high EQW and low LCD, the match with the set of profiles with inner velocity set equal to zero were found to be the best. So the velocity at the inner edge, V_a, was chosen to be zero for the final matching of the observed profiles. The outer velocity was varied from 0 to 9 thermal units. A few representative computed profiles are shown in Fig. 7.

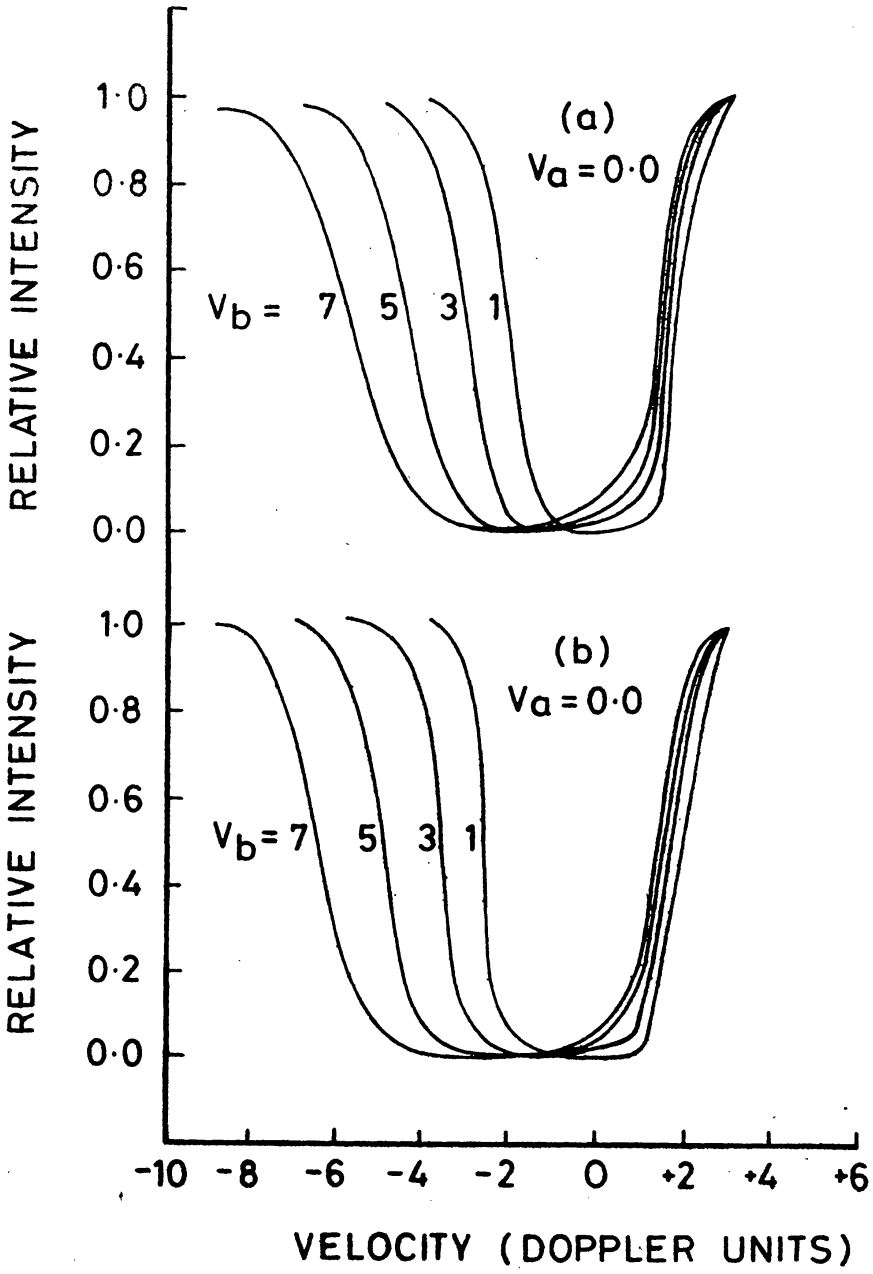

Figure 7. Computed profiles for (a) $\tau=30$ and (b) $\tau=80$. V_a and V_b are the velocities (in Doppler units) at the inner and the outer radius.

3.6 *Results*

Optical depths and velocities

To obtain the optical depth in the H_α line and the velocity structure of the region where the H_α line is formed in these stars, the following procedure was adopted.

The LCD is a function of V_b and τ for a given ξ_t and ΔR (Fig. 8). With increasing V_b the LCD also increases. In general, the LCD increases also with τ, for, a larger optical depth implies that only the outermost layers are seen where the velocities are higher. For the lower optical depths the LCD increases almost linearly with V_b till $V_b \simeq 3{\cdot}0$ beyond which the variation slows down so that the LCD becomes almost independent of V_b. Beyond $\tau = 15$, the LCD – V_b relation is linear over a much larger range of V_b and practically independent of τ.

The EQW is also a function of τ and V_b for a given ξ_t and ΔR (Fig. 9). Increase of V_b stretches the line profile over a larger width in the continuum and a higher EQW is obtained. The EQW increases almost linearly with τ for small values of τ, then there is a change of slope around $\tau = 25$ and for higher values of τ, it is a relatively slowly-varying function. It might be worth noting that this is analogous to the linear and saturated regions of the classical curve of growth.

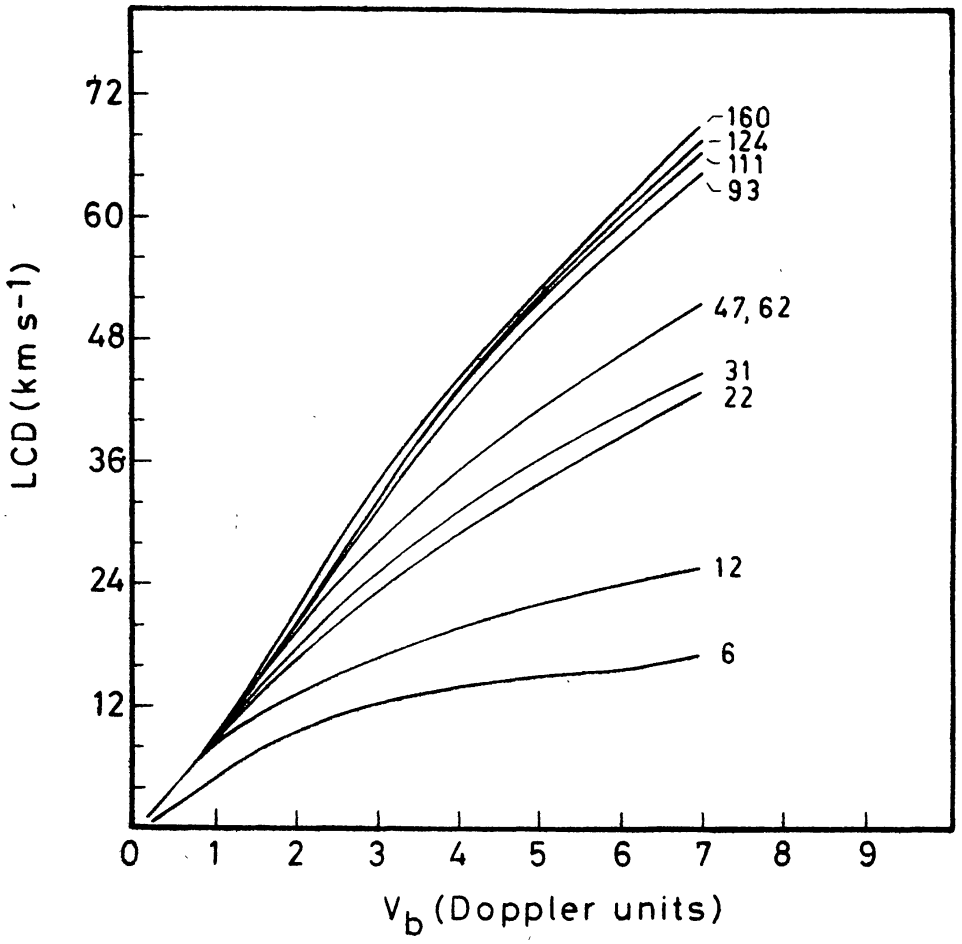

Figure 8. The computed line-core displacement versus outer velocity for $\xi_t = 15$ km s^{-1}. Each curve is labelled by the optical depth, τ.

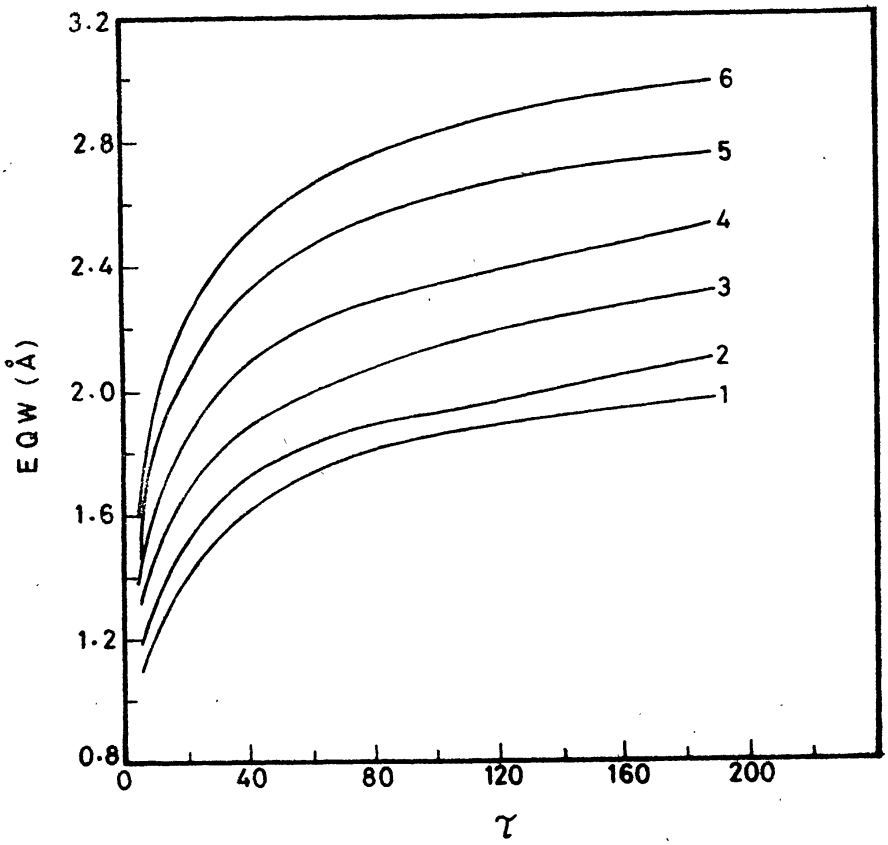

Figure 9. The computed equivalent width versus optical depth for ξ_t=15 km s^{-1}. Each curve is labelled by the outer velocity V_b.

The final solution of obtaining τ and V_b through a match of the observed and the computed profiles was effected graphically. For a particular star, the observed LCD gives a set of (τ, V_b) solutions on the LCD – V_b graph. The observed EQW also gives a set of (τ, V_b) solutions on the EQW – τ plot. The uniqueness of the solution requires that just one (τ, V_b) combination should be common to both while the rest are discrepant. Such a unique solution was indeed found for sixteen stars which have EQW $\geqslant$ 1·6Å and LCD $\geqslant$ — 12 km s^{-1}. However, for stars with lower EQW and/or higher LCD a certain ambiguity crept in. It was seen that more than one (τ, V_b) combination satisfied the observed EQW and LCD. In particular, for these stars, proper matching could be obtained with either a high V_b and low τ or a low V_b and high τ. In order to resolve this ambiguity, some other observed characteristic of the line had to be used. An important parameter used commonly in the Ca II H and K and Mg II h and k studies of late-type stars is the asymmetry of the line profile (Stencel 1978; Stencel and Mullan 1980). In the present work a similar asymmetry parameter for the H_α line was used. If a line is drawn through the displaced line minimum perpendicular to the direction of dispersion, then the asymmetry γ may be defined as the ratio of the flux to the shortward side of this line to the flux to its longward side, *i.e.* $\gamma = f_-/f_+$. In the observed line profiles, γ is always less than 1·0, ranging from 0·6 to 0·9. In the theoretical profiles, on the other hand, γ varies from 0·5 to 2.2. For the stars for which more than one (τ, V_b) combination was obtained, it was found that the low τ – high V_b set always gave a γ greater than 1, while the other solution fit well with the observed profile. Incidentally, for stars for which unique

Table 3. Optical depths, kinematics and mass-loss rates.

Star	$\Delta R = 1.0 \times 10^{13}$cm, $\xi_t = 10$ km s^{-1}					$\xi_t = 15$ km s^{-1}				
	V_b km s^{-1}	τ	$\bar{V}$ km s^{-1}	N cm^{-2}	$\dot{M}$ $M_\odot$ yr^{-1}	V_b km s^{-1}	τ	$\bar{V}$ km s^{-1}	N cm^{-2}	$\dot{M}$ $M_\odot$ yr^{-1}
HD 77912	24·5	63	5·0	7·20(+22)	1·61(−6)	25·3	13	5·2	1·98(+22)	4·60(−7)
ϵ Gem	15·9	500	3·3	5·75(+23)	8·35(−6)	15·4	68	3·1	1·04(+23)	1·45(−6)
33 Sgr	11·3	400	2·3	4·60(+23)	4·72(−6)	10·2	49	2·1	7·50(+22)	6·90(−7)
ζ Cep	25·0	375	5·0	4·32(+23)	9·73(−6)	24·4	69	4·9	1·05(+23)	2·29(−6)
HD 196093	36·7	34	7·3	3·90(+22)	1·27(−6)	33·1	12	6·6	1·80(+22)	5·30(−7)
ϵ Peg	16·5	530	3·3	6·10(+23)	9·10(−6)	17·1	75	3·4	1·14(+23)	1·75(−6)
η Per	14·6	570	3·0	6·56(+23)	8·64(−6)	14·5	86	2·7	1·31(+23)	1·60(−7)
HD 17958	36·1	25	7·1	2·90(+22)	9.20(−7)	34·5	9	7·3	1·40(+22)	4·60(−7)
o^1 CMa	13·8	50	2·7	5·80(+22)	6·90(−7)	14·5	10	3·4	1·50(+22)	2·30(−7)
41 Gem	17·1	95	3·4	1·09(+23)	1·67(−6)	17·1	18	3·2	2·70(+22)	3·80(−7)
HD 56577	11·0	203	2·2	2·34(+23)	2·30(−6)	12·5	26	2·6	4·00(+22)	4·60(−7)
HD 62576	32·0	28	6·5	3·20(+22)	9·20(−7)	30·4	10	5·7	1·50(+22)	3·80(−7)
HD 68553	49·6	39	10·0	4·50(+22)	2·02(−6)	53·4	12	10·4	1·80(+22)	8·40(−7)
HD 80108	38·2	165	7·7	1·90(+23)	6·57(−6)	44·4	24	8·8	3·70(+22)	1·45(−6)
HD 91056	16·5	710	3·3	8·17(+23)	1·22(−5)	17·1	198	3·4	3·02(+23)	4·58(−6)
β Ara	30·8	200	6·2	2·30(+23)	6·39(−6)	34·8	27	7·1	4·10(+22)	1·30(−6)
HD 4817	22·0	377	4·5	4·34(+23)	8·64(−6)	21·7	77	4·4	1·17(+23)	2·29(−6)
λ Vel	21·4	269	4·3	3·10(+23)	5·99(−6)	21·5	47	4·3	7·20(+22)	1·37(−6)
HD 89388	40·4	233	8·2	2·68(+23)	9·79(−6)	48·6	30	9·6	4·60(+22)	1·98(−6)
HD 137709	17·1	420	3·5	4·83(+23)	7·49(−6)	17·1	52	3·5	7·90(+22)	1·22(−6)
ξ Cyg	17·1	570	3·5	6·56(+23)	1·02(−5)	17·1	155	3·4	2·36(+23)	3·59(−6)
σ CMa	18·8	365	3·8	4·20(+23)	7·14(−6)	20·1	58	4·1	8·80(+22)	1·60(−6)
HD 216946	29·4	340	6·0	3·91(+23)	1·04(−5)	32·1	61	6·4	9·30(+22)	2·67(−6)

solutions were already obtained without invoking the third parameter, the asymmetry of the matched profile was found to be always close to that of the observed profile. The above analysis was repeated for the other value of ξ_t. The final solutions are tabulated in Table 3.

Mass-loss rates

In a region with a specified density and velocity distribution, an average velocity $\overline{V}$ may be defined as

$$\overline{V} = \int_{R_{\rm in}}^{R_{\rm out}} n(r)\, v(r)\, dr \Big/ \int_{R_{\rm in}}^{R_{\rm out}} n(r)\, dr. \tag{8}$$

If the distribution of matter is uniform throughout the line-forming region, then with $v(r) = 0$ at $R_{\rm in}$ and $v(r) = V_b$ at $R_{\rm out}$, we have $\overline{V} = V_b/2$. Since in the present case the density goes down linearly, the more general definition of $\overline{V}$ given in Equation (8) has been adopted. The computed values of $\overline{V}$ are displayed in Columns (4) and (9) of Table 3.

The rate of mass outflow from the atmosphere can be calculated from the steady state flow condition where

$$\begin{aligned} \dot{M} &= 4\pi\, r^2\, \rho(r)\, v(r) \\ &= 4\pi\, m_{\rm H}\, (1 + \eta)\, r^2\, n(r)\, v(r). \end{aligned} \tag{9}$$

Here $m_{\rm H}$ is the mass of the H-atoms and η, the relative abundance by weight of the elements heavier than hydrogen. The value of η was adopted from Bell *et al.* (1976) and is equal to 0·42 for a standard Population I composition. The inner radius of the line-forming region which is taken to be the radius of the star in the present work, enters directly into the mass-loss calculations. An error in $R_{\rm in}$ results in a proportionately large error in the mass-loss rate.

If the above variables are replaced by their average values, then the mass-loss rate in the present model can be written as

$$\dot{M} = 4\pi\, m_{\rm H}\, (1 + \eta)\, R_{\rm in}^2 \left(1 + \frac{\Delta R}{R_{\rm in}}\right) \frac{N}{\Delta R}\, \overline{V} \tag{10}$$

where N is the column density and all other quantities have been defined previously. The column densities obtained from Equation (7) are listed in Columns (5) and (10) of Table 3. Using the values of N and $\overline{V}$, the mass-loss rate was evaluated for all the programme stars for each ξ_t. As can be seen, the mass-loss rates lie in the range of $10^{-6} - 10^{-7}\ M_\odot\ {\rm yr}^{-1}$, higher than the empirical mass-loss relation derived by Reimers (1973). Since the assumption of a particular value of ξ_t affects the value of the column density derived, the mass-loss rates are slightly different, being lower for the higher value of microturbulence by a factor of 5 or so.

In order to produce strong absorption cores, the source function, in general, has to drop rapidly enough (by several orders of magnitude) across the line-forming region. The combination of a constant velocity and a density decreasing as the square of the distance has been widely used in the study of circumstellar envelopes (Weymann 1962; Sanner 1976; Bernat 1977; Hagen 1978). The resultant source function produces profiles with a P Cygni-type appearance. Even in a geometrically thin atmosphere, the red-side emission which is small for low optical depths tends to increase dramatically as the optical depth goes up, resulting in typical P Cygni profiles. This combination of density and velocity will, therefore, never yield profiles to match the observed characteristics of the H_α line.

With a linearly decreasing density and velocity in a pure scattering medium ($\epsilon = \beta = 0$), the line source function drops down by several orders of magnitude over the extent of the line-forming region (Peraiah 1981). A model envelope with these properties could, in principle, be used to generate deep absorption profiles. A preliminary analysis showed that to obtain EQW in the range of the observed values, a large spread in the velocity was generally required. This requirement could only be fulfilled when the inner velocity was chosen to be sufficiently large. Since most of the absorbing material was also located near the inner edge in this model, the LCD became inordinately large. The observed high EQW and low LCD could thus never be matched simultaneously. On the contrary, the model envelope adopted in the present analysis has a linearly decreasing density and a positive velocity gradient. The resulting source function is low enough to produce the strong absorption cores. At the same time, a large velocity spread satisfying the observed high EQW's requires a low velocity at the inner edge and a low LCD is obtained as a result. Therefore, the observed EQW and LCD could be matched simultaneously. In this last case, the equation of continuity is strictly satisfied only in the limit of a plane-parallel geometry. This is not inconsistent since we have also assumed the line-forming region to extend over only a fraction of the stellar radius. With the velocity increasing outward, a model, in strict spherical symmetry, requires a density law $n(r) \propto r^{-3}$. Calculations of the line source function and the H_α line profiles with this density distribution are in progress.

4. Discussion

In the present work, we have tried to model the H_α absorption line in G and K supergiants. The observed asymmetry in H_α has been attributed to the presence of an outward flow in the chromospheres of these stars. A predetermined source function was used to generate the H_α line profiles. The best description of the H_α-forming region is provided by a case of linearly increasing velocity and decreasing density. The theoretical profiles computed with this particular combination of $n(r)$ and $v(r)$ have then been matched with the observed profiles to obtain the column densities and velocities of the H_α-forming regions. Finally, mass-loss rates from the expanding chromospheres have been derived assuming a steady flow.

No other determination of mass-loss rates of G and K supergiants exists except for two of them, namely, η Per and HD 216946. Reimers (1973) calculated on the basis of their Ca II K emission shifts, mass-loss rates on the order of $2 \times 10^{-7}\ M_\odot$ yr^{-1}. These are almost one order of magnitude lower than the values quoted in our

Table 3. The situation is different for M giants and supergiants. Following the pioneering work of Deutsch (1956, 1960), a large number of studies has been devoted to the circumstellar envelopes of these stars and a sizable literature on the mass-loss rates exists for these (Weymann 1962; Sanner 1976; Bernat 1977; Hagen 1978). The mass-loss rates determined by all these investigators fall in the range of $10^{-4}-10^{-8}$ $M_\odot$ yr^{-1}. Since these studies refer specifically to the circumstellar envelopes, the velocities obtained from the blueshifted absorption cores of the lines are treated as true terminal velocities of expansion. The rates obtained by Bernat (1977) are the highest yet calculated, a consequence of the very large inner radii he adopted for the circumstellar envelopes. Very recently, VLA observations of OH maser emission at 1612 MHz in the circumstellar envelopes of twenty very red giants and supergiants have become available (Bowers, Johnston and Spencer 1981). The observed expansion velocities have been used to derive mass-loss rates in the range of $10^{-4}-10^{-6}$ $M_\odot$ yr^{-1}. The OH emission comes from regions far out in the envelope where the gas has already reached a terminal velocity. Therefore, these observations provide a very accurate way of knowing $V_{\rm exp}$ and hence of determining mass-loss rates. The G, K and early M supergiants do not show any maser emission (Cassinelli 1979). These stars do not show any detectable free-free radio emission either. Therefore, the mass-loss rates derived here cannot be directly compared.

The phenomenon of the stellar wind which is responsible for the loss of mass from stars is not confined only to the very outer layers of the atmosphere. It reaches as deep as the chromosphere as indicated by the blueshifts of Ca II K_2 (Stencel 1978) and the H_α asymmetries (Boesgaard and Hagen 1979). The presence of blueshifted cores of H_α in G and K supergiants studied here also shows that expansion occurs within the chromosphere itself. Mullan (1978) proposed that when the sonic point of a stellar wind lies very close to the chromosphere-corona transition region, the chromospheric gas itself starts participating in the expansion. He derived a supersonic transition locus (STL) on the HR diagram along which the chromospheric expansion is expected to set in. Because of the access of the wind to the chromospheric material, there is a sudden increase in the mass flux as the higher density material starts participating in the expansion and hence stars to the right of the STL are expected to have enhanced mass-loss rates. A number of observations lend support to the idea of the theoretical STL—(a) The STL matches quite well with the observational boundary of the large mass-loss regime determined by Reimers (1977). (b) The Ca II asymmetry dividing line discovered by Stencel (1978) also lies very close to the STL. Stencel and Mullan (1980) have further used the IUE observations of the Mg II resonance lines ($\lambda\lambda$ 2796, 2803) and located a boundary on the HR diagram where these lines change the sense of their asymmetry in the same way as the Ca II. Since Mg II is formed at greater heights in the chromosphere, the boundary where these lines change the sense of asymmetry lies to the left of the corresponding dividing line for Ca II. (c) Linsky and Haisch (1979) have discovered from the IUE observations of late-type stars, a temperature dividing line which is very close to Mullan's STL. According to them, stars to the left of the dividing line have very hot coronae and hardly lose any mass. On the other hand stars to the right have cool coronae and large expanding chromospheres.

There are indications from the last study that at least two of our programme stars belong to the large mass-loss regime. Both ϵ Gem (G8 Ib) and λ Vel (K5 Ib) have been observed by IUE (Linsky and Haisch 1979; Hartmann, Dupree and Raymond

1980). Their spectra contain chromospheric lines like L_α, Si II, C I, O I but no lines arising from the higher stages of ionization, *e.g.* He II, C II–C IV, Si III–Si IV, Nv, usually found in the transition region between the chromosphere and the corona. ϵ Gem and λ Vel fall to the right of the temperature dividing line on the HR diagram. It is hoped that as more UV observations of G and K supergiants become available in future, many more of our programme stars will be found to belong to the class of stars having cool coronae and large mass loss.

The Ca II and the Mg II lines are the most extensively studied features of the chromospheres. Their structures are very similar to each other. First, due to the temperature rise in the chromosphere, the K_2 (or k_2) emission component appears within the main absorption profile and then a further central absorption reversal K_3 (or k_3) occurs in the chromosphere and the circumstellar envelope. In cool supergiants like ϵ Gem (G8 Ib), ϵ Peg (K2 Ib) and ξ Cyg (K5 Ib), the circumstellar absorption completely masks the Ca II and Mg II line asymmetries (Linksy *et al.* 1979; Basri and Linsky 1979). Therefore, it is difficult to disentangle the asymmetric chromospheric line. Also the Mg II k line profile is blended with circumstellar Fe II and Mn I absorption lines (Bernat and Lambert 1976; de Jager *et al.* 1979). The H_α line is essentially free of such complications and, therefore, serves as a more efficient indicator of the conditions in the chromosphere itself.

Because of the complex nature of the composite line profiles of Ca II and Mg II, with different parts originating in different regions of the atmosphere, it is very difficult to describe uniquely the velocity patterns with the help of either Ca II or Mg II when differential motions are present. For example, downward motions in the K_3-forming region and no detectable motion in the K_2-forming region yield similar line asymmetries as upward motions in the K_2-forming region with no detectable motion in the K_3-forming region. Thus the observed asymmetry does not provide information about the magnitude or the direction of flow in any particular region. On the other hand, H_α has the bulk of its absorption in the chromosphere and has no circumstellar contribution. Being a photoionization controlled line in late-type stars, it is a pure absorption profile with no emission reversal. As a result, the observed blueshift of the absorption core can be non-ambiguously interpreted as indicative of an outward flow of the gas.

By using the H_α line alone, only the column density is obtained uniquely. Therefore, a definite determination of the extent of the expanding chromosphere is not possible. The derived mass-loss rates are to be treated as approximate in the light of the various uncertainties involved. Most importantly, the mechanism by which the second level of hydrogen is populated is not well understood. A realistic estimate of δ in Equation (7) is thus not possible at present. This alone may lead to an error of $\pm$ 2 orders of magnitude. The mass-loss rate is also crucially dependent upon R_{in}, which in this case is the radius of the star. For lack of direct observations of R_{in}, we have calculated R_{in} from $L = 4\pi R^2 \sigma T_{eff}^4$, knowing M_{bol} and T_{eff} from observations. This was used in Equation (10) to obtain $\dot{M}$. An error in R_{in} would produce a proportionately large error in $\dot{M}$. However, it seems unlikely that the value of R_{in} used here is off by more than a factor of 2 or 3. Further, since line profile asymmetries are the only means at present of studying chromospheric velocity fields, any discussion of mass outflow from the chromosphere leans heavily on an

average velocity (*e.g.* $\bar{V}$ as in Equation 8). The limitations of using such an average should be kept in mind.

Several improvements on the present analysis are possible which future investigations may incorporate. Since H_α in late-type stars is a photoionization-dominated line, the effect of the continuum together with several levels should be included in a full discussion of the line-formation problem. In using a two-level atom, we have assumed the presence of detailed balance in the Lyman lines. It is now known that in the Sun, detailed balance in L_α may be an erroneous assumption. The formation of L_α itself has to be included in an accurate discussion of the H_α line. The L_α source function sensitively depends upon the redistribution function and since the optical depth in H_α is directly proportional to the population of the $n = 2$ level of H, it is determined by the L_α source function (Athay 1976). In the chromospheres of supergiants, where the densities are much lower, the L_α source function will be greatly affected by partial redistribution of photons and the formation of the H_α line becomes further complicated.

We have used the H_α source function with $\epsilon = 0$ and $\beta = 0$. With $\beta = 0$, the computed line profiles have highly saturated and wide cores. The use of a small but nonzero value of β in the source function would raise the core, resulting in computed profiles that are very similar in appearance to the observed profiles.

It is strongly suspected that there are very small emission components lying above the continuum level either to the left or to the right of the absorption profile in several of the stars studied here. A more widened spectrum of each star with better signal-to-noise ratio would depict such components more easily. While the presence of only red-side emission is a direct consequence of the extended geometry of the situation, both blue and red emission can be explained if one assumes the existence of an extended circumstellar shell—a few stellar radii away—at a higher velocity. The presence of red- and blueshifted emission with respect to the H_α absorption core in bright red giants of several globular clusters has in general been attributed to circumstellar envelopes (Cohen 1976; Reimers 1977; Mallia and Pagel 1978; Cacciari and Freeman 1981). If the reality of these emissions is clearly established for the stars under study, they may be used to probe the very outermost layers of these stars and yield further valuable information on the stellar winds associated with them.

Acknowledgements

This paper is based on a doctoral thesis submitted to the Madurai Kamaraj University. I am most grateful to Professor M. K. V. Bappu for his supervision and wise counsel throughout the course of this work. I am also indebted to him for generous allotment of observing time. I am especially thankful to A. Peraiah for allowing me to use his radiative transfer code and also for his help in the computational aspects of the problem. I have particularly benefited from several stimulating discussions with D. C. V. Mallik. It is also a great pleasure to thank M. H. Gokhale and P. Venkatakrishnan for helpful comments. I also thank an anonymous referee for valuable comments and for clarifying a few conceptual difficulties. This work was supported by the National Council of Educational Research and Training and the Indian Institute of Astrophysics.

References

Athay, R. G. 1976, *The Solar Chromosphere and Corona: Quiet Sun*, D. Reidel, Dordrecht.
Athay, R. G., Thomas, R. N. 1958, *Astrophys. J.*, **127**, 96.
Ayres, T. R., Linsky, J. L. 1975, *Astrophys. J.*, **200**, 660.
Bappu, M. K. V. 1981, *Bok Festschrift*, Ed. R. E. White (in press).
Basri, G. S., Linsky, J. L. 1979, Astrophys. J., **234**, 1023.
Bell, R. A., Eriksson, K., Gustafsson, B., Nordlund, A. 1976, *Astr. Astrophys. Suppl. Ser.*, **23**, 37.
Bernat, A. P. 1977, *Astrophys. J.*, **213**, 756.
Bernat, A. P., Lambert, D. L. 1976, *Astrophys. J.*, **204**, 830.
Bidelman, W. P. 1954, *Astrophys. J. Suppl. Ser.*, **1**, 175.
Boesgaard, A. M., Hagen, W. 1979, *Astrophys. J.*, **231**, 128.
Bowers, P. F., Johnston, K. J., Spencer, J. H. 1981, *Nature*, **291**, 382.
Cacciari, C., Freeman, K. C. 1981, in *Physical Processes in Red Giants*, Eds I. Iben, Jr. and A. Renzini, D. Reidel, Dordrecht, p. 311.
Cassinelli, J. P. 1979, *A. Rev. Astr. Astrophys.*, **17**, 275.
Cohen, J. 1976, *Astrophys. J.*, **203**, L127.
de Jager, C., Kondo, Y., Hoekstra, R., van der Hucht, K. A., Kamperman, T. M., Lamers, H. J. G. L. M., Modisette, J. L., Morgan, T. H. 1979, *Astrophys. J.*, **230**, 534.
Deutsch, A. J. 1956, *Astrophys. J.*, **123**, 210.
Deutsch, A. J. 1960, in *Stellar Atmospheres*, Ed. J. L. Greenstein, University of Chicago Press, p. 543.
Goldberg, L. 1979, *Q. J. R. astr. Soc.*, **20**, 361.
Hagen, W. 1978, *Astrophys. J. Suppl. Ser.*, **38**, 1.
Hartmann, L., Dupree, A. K., Raymond, J. C. 1980, *Astrophys. J.*, **236**, L143.
Hoffleit, D. 1964, *Catalogue of Bright Stars*, Yale University Observatory, New Haven.
Humphreys, R. M. 1970, *Astr. J.*, **75**, 602.
Jefferies, J., Thomas, R. 1959, *Astrophys. J.*, **129**, 401.
Johnson, H. L. 1966, *A. Rev. Astr. Astrophys.*, **4**, 193.
Joy, A. H., Wilson, R. E. 1949, *Astrophys. J.*, **109**, 231.
Kraft, R. P., Preston, G. W., Wolff, S. C. 1964, *Astrophys. J.*, **140**, 235.
Kuhi, L. V. 1974, in *Highlights of Astronomy*, Vol. 3, Ed. G. Contopoulos, D. Reidel, Dordrecht, p. 121.
Kunasz, P. B., Hummer, D. G. 1974, *Mon. Not. R. astr. Soc.*, **166**, 57.
Linsky, J. L. 1980, *A. Rev. Astr. Astrophys.*, **18**, 439.
Linsky, J. L., Haisch, B. M. 1979, *Astrophys. J.*, **229**, L27.
Linsky, J. L., Worden, S. P., McClintock, W., Robertson, R. M. 1979, *Astrophys. J. Suppl. Ser.*, **41**, 47.
Luck, R. E. 1977, *Astrophys. J.*, **212**, 743.
Luck, R. E. 1979, *Astrophys. J.*, **232**, 797.
Mallia, E. A., Pagel, B. E. J. 1978, *Mon. Not. R. astr. Soc.*, **184**, 55 p.
Mihalas, D. 1978, *Stellar Atmospheres*, 2nd edn, Freeman, San Francisco.
Mullan, D. J. 1978, *Astrophys. J.*, **226**, 151.
Peraiah, A. 1979, *Astrophys. Sp. Sci.*, **63**, 267.
Peraiah, A. 1980, *J. Astrophys. Astr.*, **1**, 101.
Peraiah, A. 1981, *Astrophys. Sp. Sci.*, **77**, 243.
Peraiah, A., Grant, I. 1973, *J. Inst. Math. Applics.*, **12**, 75.
Reimers, D. 1973, *Astr. Astrophys.*, **24**, 79.
Reimers, D. 1975, in *Problems in Stellar Atmospheres and Envelopes*, Eds B. Baschek, W. H. Kegel and G. Traving, Springer-Verlag, New York, p. 229.
Reimers, D. 1977, *Astr. Astrophys.*, **57**, 395.
Sanner, F. 1976, *Astrophys. J. Suppl. Ser.*, **32**, 115.
Stencel, R. E. 1978, *Astrophys. J.*, **223**, L37.
Stencel, R. E., Mullan, D. J. 1980, *Astrophys. J.*, **238**, 221.
Warner, B. 1966, *Observatory*, **86**, 82.
Warner, B. 1968, *Observatory*, **88**, 217.
Warner, B. 1969, *Mon. Not. R. astr. Soc.*, **144**, 333.

Weymann, R. 1962, *Astrophys. J.*, **136**, 844.
Wiese, W. L., Smith, M. W., Glennon, B. M. 1966, *Atomic Transition Probabilities*, Vol. 1, Nat. Bur. Stand., (U.S.).
Wilson, O. C. 1976, *Astrophys. J.*, **205**, 823.
Wilson, O. C., Bappu, M. K. V. 1957, *Astrophys. J.*, **125**, 661.